https://doi.org/10.2352/ISSN.2470-1173.2018.8.MAAP-168

A General Method for Estimating Fluorescent Donaldson Matrices

Shoji Tominaga[1,2], Keita Hirai[1], Takahiko Horiuchi[1]
[1]Graduate School of Engineering, Chiba University, Chiba, Japan
[2]Department of Computer Science, Norwegian University of Science and Technology, Gjøvik, Norway

Abstract

The present paper proposes a generalized method to estimate the bispectral Donaldson matrices of fluorescent objects. We suppose that the matte surface of a fluorescent object is illuminated by each of light sources with different spectral-power distributions, and is observed by a spectral imaging system in a visible wavelength range. The Donaldson matrix is decomposed into three spectral functions of reflection, fluorescent excitation and fluorescent emission. We segment the visible wavelength into two ranges having (1) only reflection without luminescence and (2) both reflection and fluorescent emission. An iterative algorithm is presented to effectively estimate the three spectral functions on the residual minimization. The wavelength range of fluorescent emission is also estimated. The proposed method is reliable in the sense that the estimates are determined to minimize the average residual error to the observations. The feasibility of the method is shown in experiments using two fluorescent samples and four illuminants.

Introduction

Use of fluorescent materials has increased in our daily lives. Many sorts of objects we see in each day are made of materials which include florescence. The attractive usefulness of fluorescence is based on the visual effect that the visual appearance of the object surface is improved, compared with a reflective object surface based on non-fluorescent light reflection. In fact, because of fluorescent emission, many fluorescent surfaces appear brighter and more vivid than the original object color surface.

The fluorescent characteristics are well described in terms of the bispectral radiance factor. The radiance factor is a function of two wavelength variables: the excitation wavelength of incident light and the emission/reflection wavelength. The bispectral radiance factor can be summarized as a Donaldson matrix [1], which is an illuminant independent matrix representation of the bispectral radiance factor of a target object. The bispectral radiance factor can be measured using two monochromators according to the definition [2]. An essential problem of the two-monochromator method is time-consuming and expensive, which its use is confined in the laboratory setup and not available in an ordinary scene using imaging system.

Recently Tominaga et al. [3] presented a method for estimating the bispectral Donaldson matrices of fluorescent objects by using only two illuminant projections. The Donaldson matrix represents the spectral radiance factor consisting of the sum of two components: a reflected radiance factor and a luminescent radiance factor, which is further separated into the emission and excitation wavelength components. This Donaldson matrix representation is useful in various fluorescence analysis like mutual illumination [4], appearance reconstruction [5], and texture analysis [6]. The two-illuminant projection method used only two sets of spectral sensor outputs under two different illuminants. The estimation principle was based on the property that the difference between the observed reflected radiance factors under the two different illuminants was not caused by the reflected radiance component, but only the luminescent radiance component. However, the method did not necessarily provide an optimal solution for the spectral estimation problem. It was restricted into use of two illuminants having continuous spectral-power distributions. We found that the estimation results were often unreliable and unstable, especially for low intensity light sources or noisy observations in the imaging system.

The present paper proposes a generalized method to estimate the bispectral Donaldson matrices of fluorescent objects. We use two and more light sources. Each illuminant is projected uniformly onto the flat surface of a fluorescent object, which is observed by a spectral imaging system with narrow band characteristics in a visible wavelength range. The Donaldson matrix is decomposed into three components of reflection, fluorescent excitation and fluorescent emission. The estimation problem of the spectral component functions is solved as an optimization problem to minimize the residual error of the observations captured by the spectral imaging system.

An iterative computational algorithm is presented to effectively estimate three spectral components of fluorescent excitation, fluorescent emission, and reflection. We segment the visible wavelength range into two types of ranges: one consisting of only reflection without fluorescent emission and another consisting of both reflection and fluorescent emission. For the former range, the reflection component is straightforwardly estimated. For the latter range, the three components are estimated iteratively to minimize the residual errors to multiple observations under different illuminants. The precise wavelength range of luminescent emission is also estimated on the residual minimization. The feasibility of the proposed method is examined in experiments using different fluorescent samples and illuminants. The estimation performance is discussed in detail.

Observation Model of a Fluorescent Object

The matte surface of a fluorescent object is illuminated uniformly by different light sources. A spectral imaging system placed in the front captures the spectral images at equal wavelength intervals in a visible range (400,700nm). The sensor outputs averaged over a flat area are acquired as spectral radiances. The same surface was also observed using a spectro-radiometer auxiliarily.

A Donaldson matrix $D(\lambda_{em}, \lambda_{ex})$ represents the bispectral radiance factor of a fluorescent object as a two-variable function of the excitation wavelength λ_{em} and the emission/reflection

wavelength λ_{ex} . The diagonal at $\lambda_{em} = \lambda_{ex}$ represents the reflected radiance factor corresponding surface-spectral reflectance $S(\lambda)$. The luminescent radiance factor by fluorescent emission is located only in the off-diagonal at $\lambda_{em} > \lambda_{ex}$ because the luminescent energy is emitted at a longer wavelength than each excitation wavelength (called Stokes shift [7]). A fluorescent object contains usually a single fluorescent material (fluorophore). In this case, the luminescent radiance factor $D_L(\lambda_{em}, \lambda_{ex})$ is separated into excitation and emission wavelength components as $D_L(\lambda_{em}, \lambda_{ex}) = \alpha(\lambda_{em})\beta(\lambda_{ex})$ (see [3]). In this separation, we assume that the excitation spectrum is normalized as $\int \beta(\lambda_{ex}) d\lambda_{ex} = 1$. The excitation range for all fluorescent materials was often assumed between about 330-350 nm and 10 nm shorter than the emission peak wavelength (see [8],[9]). The lower limit in this paper is set to 350 nm.

Let $E(\lambda)$ be the illuminant spectrum of a light source. The observations of spectral radiances are described as

$$\begin{aligned} y(\lambda_{em}) &= S(\lambda_{em})E(\lambda_{em}) + \alpha(\lambda_{em}) \int_{350}^{\lambda_{em}} \beta(\lambda_{ex})E(\lambda_{ex}) d\lambda_{ex} \\ &= S(\lambda_{em})E(\lambda_{em}) + \alpha(\lambda_{em})C(\lambda_{em}), \end{aligned} \tag{1}$$

where

$$C(\lambda_{em}) = \int_{350}^{\lambda_{em}} \beta(\lambda_{ex})E(\lambda_{ex}) d\lambda_{ex}. \tag{2}$$

The right two terms in Eq.(1) represent, respectively, the diffuse reflection component and the fluorescent emission component.

Most imaging systems operate only in the visible wavelength range (400, 700 nm). On the other hand, it is possible that the excitation of fluorescent material is caused in the entire range (350, 700 nm) of the illuminant. Therefore, the Donaldson matrix is estimated in a rectangular matrix form corresponding to (400, 700 nm) × (350, 700 nm) . A discrete form of the Donaldson matrix with the above properties can be represented in an $N \times M$ matrix as

$$\mathbf{D} = \mathbf{D}_R + \mathbf{D}_L = \begin{bmatrix} \alpha_1\beta_1 & \cdots & \alpha_1\beta_{M-N} & s_1 & 0 & \cdots & 0 \\ \alpha_2\beta_1 & & \alpha_2\beta_{M-N} & \alpha_2\beta_{M-N+1} & s_2 & \ddots & \vdots \\ \vdots & & \vdots & \vdots & \ddots & \ddots & 0 \\ \alpha_N\beta_1 & \cdots & \alpha_N\beta_{M-N} & \alpha_N\beta_{M-N+1} & \cdots & \alpha_N\beta_{M-1} & s_N \end{bmatrix}, \tag{3}$$

where s_i (i = 1, 2, .., N), α_i (i=1, 2, .., N), and β_i (i = 1, 2, .., M-1) represent, respectively, the reflected radiance factor, the emission spectrum, and the excitation spectrum. When the visible range is sampled in equal intervals of 5 nm, the Donaldson matrix of Eq.(3) is written as a 61×71 matrix. Figure 1 demonstrates the Donaldson matrix of a pink sample containing an orange fluorescent color.

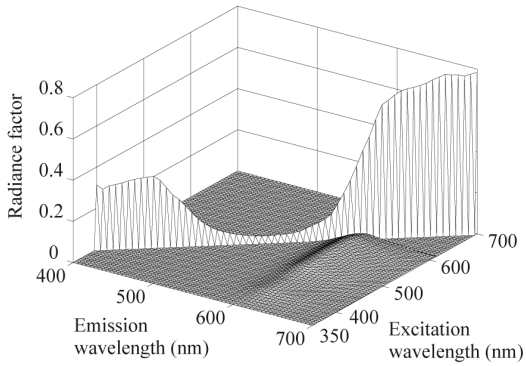

Figure 1. Donaldson matrix obtained from a pink sample containing an orange fluorescent color.

Conventional Method to Donaldson Matrix Estimation

The estimation of emission spectrum is a key step in solving the estimation problem. When the sensor outputs are divided by the known illuminant spectrum, the apparent spectral reflected radiance factor is calculated as (see [3])

$$S^*(\lambda) = y(\lambda) / E(\lambda) \tag{4}$$

Figure 2 demonstrates the apparent reflected radiance factors $S^{*(1)}(\lambda)$ and $S^{*(2)}(\lambda)$ of a green fluorescent sample observed under an incandescent lamp and an artificial sunlight lamp. The apparent reflected radiance factors are not independent of illuminants, but include the influence of fluorescent emission. In Figure 2, the apparent reflected radiance factor under the incandescent illumination is less than the sunlight because the incandescent light source has low spectral energy in the excitation region of the fluorescent sample. Note that the apparent reflected radiance factors for a non-fluorescent object are coincident as $S^{*(1)}(\lambda) = S^{*(2)}(\lambda)$. Therefore, a difference between the two apparent reflected radiance factors corresponds to the luminescent component by fluorescent emission. In Figure 2, the fluorescent emission ranges roughly from λ_1 to λ_2 . The wavelength λ_p represents the peak position of the apparent reflected radiance factor. If we know the emission range (λ_1 , λ_2 nm), the emission spectrum can be estimated in the following fashion:

$$\alpha_i = \gamma_i (s_i^{*(2)} - s_i^{*(1)}) \qquad (i = 2, 3, \ldots, N) \tag{5}$$

where the coefficients γ_i are calculated in advance using the illuminant spectra and the excitation spectrum. The above calculation is performed only in the effective region influenced by the fluorescent emission.

The conventional method includes some limitations. First, it is difficult to clearly determine the emission range (λ_1 , λ_2) numerically and even graphically as demonstrated in Figure 2. Especially, the apparent reflected radiance factors are noisy in such cases as low intensity light sources or noisy sensor outputs. Second, since the estimation is based on the difference of two apparent reflected radiance factors, light sources are restricted to only two illuminant having continuous spectral distributions. The ambiguity

of the emission range and the less reliability of the observations lead to less reliability and stability of the estimation results.

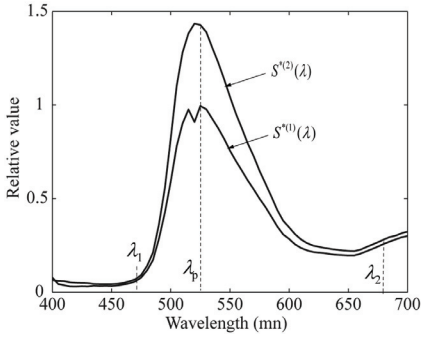

Figure 2 Apparent reflected radiance factors of a green fluorescent sample observed under an incandescent lamp ($S^{*(1)}(\lambda)$) and an artificial sunlight lamp ($S^{*(2)}(\lambda)$).

Proposed Estimation Method

We consider a general method to estimate the Donaldson matrix. We use more than or equal to two light sources. The estimation problem of the spectral component functions constructing the Donaldson matrix is solved as an optimization problem to minimize the residual error of the observations captured by the spectral imaging system.

Suppose that n light sources are available. Then the observation equations for the same fluorescent object are expressed as

$$\begin{bmatrix} y_1(\lambda) \\ y_2(\lambda) \\ \vdots \\ y_n(\lambda) \end{bmatrix} = \begin{bmatrix} E_1(\lambda) \\ E_2(\lambda) \\ \vdots \\ E_n(\lambda) \end{bmatrix} S(\lambda) + \begin{bmatrix} C_1(\lambda) \\ C_2(\lambda) \\ \vdots \\ C_n(\lambda) \end{bmatrix} \alpha(\lambda) \tag{6}$$

or equivalently

$$\mathbf{y}(\lambda) = \mathbf{E}(\lambda)S(\lambda) + \mathbf{C}(\lambda)\alpha(\lambda) \tag{7}$$

We note that the effective range of fluorescent emission is narrow in the visible range, and the wavelength range may be roughly estimated by separate ways such as use of a UV light source to illuminate the target object and/or use of the apparent reflected radiance factors which were described in the previous section. If we assume the emission range (λ_1 , λ_2), we segment the visible range (400, 700 nm) into two types of ranges: one consisting of only reflection without fluorescent emission and another consisting of both reflection and fluorescent emission. Separate estimation procedures are then devised in the respective ranges, so that the whole estimation algorithm is effective and simplified.

Let (λ_1 , λ_2) be the effective wavelength range of fluorescent emission. In the wavelength range of $400 \le \lambda < \lambda_1$ and $\lambda_2 < \lambda \le 700$, we have

$$\mathbf{y}(\lambda) = \mathbf{E}(\lambda)S(\lambda). \tag{8}$$

In these ranges, the least squares estimate of the reflected radiance factor (spectral reflectance) is obtained straightforwardly as

$$\begin{aligned} \hat{S}(\lambda) &= (\mathbf{E}^t(\lambda)\mathbf{y}(\lambda)) \Big/ (\mathbf{E}^t(\lambda)\mathbf{E}(\lambda)) \\ &= (\sum_{i=1}^{n} E_i(\lambda) y_i(\lambda)) \Big/ (\sum_{i=1}^{n} E_i^2(\lambda)), \end{aligned} \tag{9}$$

where the symbol t represents matrix transposition. The illuminant spectra $E_i(\lambda)$ (i = 1, 2, ..., n) were determined using a sample of standard white reference whose surface-spectral reflectance was known. The white reference sample was placed in the same position as the target object and illuminated with different light sources. The sensor outputs under the respective light sources, calibrated by the white reference, were used as the illuminant spectra.

In the wavelength range $\lambda_1 \le \lambda \le \lambda_2$, we have

$$\begin{aligned} \mathbf{y}(\lambda) &= \begin{bmatrix} \mathbf{E}(\lambda) & \mathbf{C}(\lambda) \end{bmatrix} \begin{bmatrix} S(\lambda) \\ \alpha(\lambda) \end{bmatrix} \\ &= \mathbf{X}(\lambda) \begin{bmatrix} S(\lambda) \\ \alpha(\lambda) \end{bmatrix} \end{aligned} \tag{10}$$

The least squares estimate of $S(\lambda)$ and $\alpha(\lambda)$ at each wavelength is obtained as

$$\begin{bmatrix} \hat{S}(\lambda) \\ \hat{\alpha}(\lambda) \end{bmatrix} = \left[\mathbf{X}^t(\lambda)\mathbf{X}(\lambda)\right]^{-1} \mathbf{X}^t(\lambda)\mathbf{y}(\lambda). \tag{11}$$

The spectral function $\mathbf{C}(\lambda)$ is calculated in a separate way using $C_i(\lambda) = \sum_j \beta(\lambda_j) E_i(\lambda_j)$. The excitation spectrum $\beta(\lambda)$ can be estimated using a physical model describing a relationship between the excitation spectrum and the reflected radiance factor

$$\beta(\lambda) = Q(\lambda)(1 - \hat{S}(\lambda)), \tag{12}$$

where $Q(\lambda)$ is the luminescence efficiency (see [3]).

We note that the spectral functions cannot be determined uniquely at once because the reflectance $S(\lambda)$ is nested in Eqs.(10) and (12). So we search iteratively the optimal estimates of the spectral functions after stating from a proper initial estimate. The initial condition of $\hat{S}(\lambda)$ is set to a constant spectrum in the excitation wavelength range. When $\hat{S}(\lambda)$ is updated at each iteration step, $\beta(\lambda)$ is estimated from Eq.(12). The predicted observations based on the estimates are described as follows:

$$\hat{\mathbf{y}}(\lambda) = \mathbf{E}(\lambda)\hat{S}(\lambda) + \hat{\mathbf{C}}(\lambda)\hat{\alpha}(\lambda). \tag{13}$$

The above procedure is repeated until the residual $\left\|\mathbf{y}(\lambda) - \hat{\mathbf{y}}(\lambda)\right\|^2$ becomes sufficiently small in the entire wavelength, where the symbol $\|\mathbf{x}\|$ represents L2 norm $\|\mathbf{x}\| = \sqrt{x_1^2 + x_2^2 + \cdots + x_n^2}$. For expressional simplicity, let $\mathbf{Y}_i$ and $\hat{\mathbf{Y}}_i$ be N-dimensional vectors

representing the spectral observation and the predicted observation under illuminant *i*. Then we use the average residual error for the entire wavelength $J = \sum_{i=1}^{n} \left\| \mathbf{Y}_i - \hat{\mathbf{Y}}_i \right\| / n$ as a performance index of the present estimation. Note that smaller the index value corresponds to better the performance. We need the spectral information of illuminant and excitation spectra in the range $350 \le \lambda < 400$ nm. Since the present spectral imaging system is not available in this range, we used the spectrometers of Ocean Optics USB-4000 and Konica Minolta CS-2000 to predict $E(\lambda)$ in $350 \le \lambda < 400$ nm. The excitation spectrum $\beta(\lambda)$ in $350 \le \lambda < 400$ nm is predicted by interpolation based on the estimates $\hat{\beta}(\lambda)$ for $\lambda \ge 400$ under the terminal condition of $\hat{\beta}(350\,\text{nm}) = 0$.

In the previous stage, we assumed (λ_1 , λ_2). So for the final stage, we determine the optimal range (λ_1 , λ_2) for effective fluorescent emission. A pair of wavelengths (λ_1 , λ_2) are two-dimensional parameters, and the optimal parameter values are determined to minimize the performance index *J*. We should note that the emission spectrum $\alpha(\lambda)$ is unimodal, which has a single peak as shown in Figure 3. In order to investigate the unimodal property, we examine the slope around the peak of the emission spectrum. The slope of the spectral function should be positive in $\lambda_1 \le \lambda < \lambda_p$ and negative in $\lambda_p < \lambda \le \lambda_2$. Thus, the estimates of (λ_1 , λ_2) are determined to satisfy the minimum index value and the unimodality.

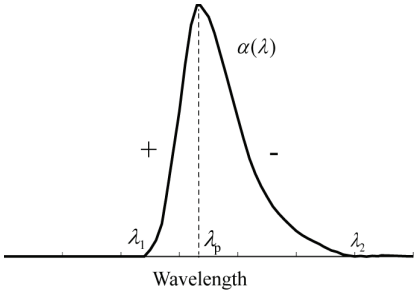

Figure 3 Unimodality of the emission spectrum.

Experimental results

The feasibility of the proposed method was examined using two fluorescent paper samples in details. These samples were illuminated by light sources with different spectral-power distributions. Figure 4 shows the spectral-power distributions for light sources of (1) an incandescent lamp (called illuminant A), (2) an artificial sunlight lamp, (3) a flood daylight lamp, and (4) a white LED lamp, used in experiments. Figure 5 shows the observed images of (a) a pink fluorescent sample and (b) a green fluorescent sample, under the four light sources. The spectral imaging system consisted of a monochrome CCD camera (Q Imaging Retiga 1300), a VariSpec LCT filter, and a personal computer. The spectral images were captured at 5 nm intervals in the visible range, so that each captured image was represented in an array of 61-dimensional vectors. A portion of the captured sample image was used in the analysis.

First, we determined the wavelength range of the effective fluorescent emission (λ_1 , λ_2). Figure 6 depicts the performance index *J* of the average residual as a function of parameters λ_1 and λ_2 in the case of the pink fluorescent sample, where λ_1 and λ_2 indicate the sample number (1, 2, …, 61) corresponding to the wavelength (400, 405, …, 700 nm). The iterative algorithm converged after about three iterations. The rectangular range in Figure 6 satisfies the unimodal property of the emission spectrum. Then the index *J* is minimized at (λ_1 , λ_2)=(34,61), so that the emission range is estimated as $34 \le \lambda \le 61$ or equivalently $565 \le \lambda \le 700$ nm .

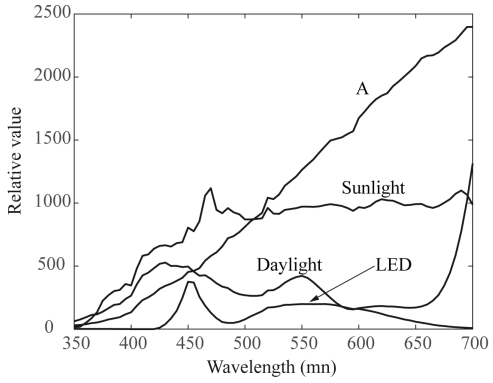

Figure 4 spectral-power distributions of (1) an incandescent lamp (A), (2) an artificial sunlight lamp, (3) a flood daylight lamp, and (4) a white LED lamp.

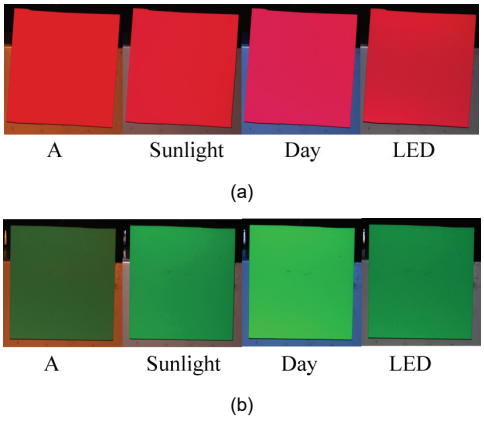

Figure 5 Observed images of (a) a pink fluorescent sample and (b) a green fluorescent sample, under four light sources.

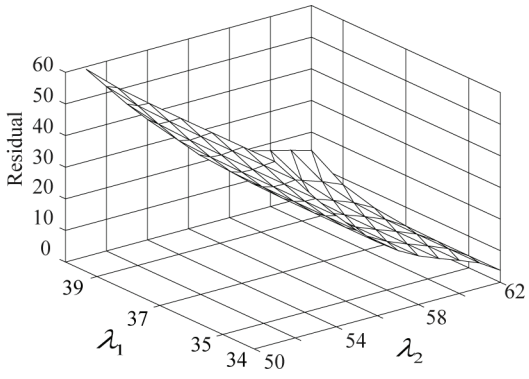

Figure 6 Performance index as a function of parameters λ_1 and λ_2 in the case of the pink fluorescent sample, where λ_1 and λ_2 indicate the sample number (1, 2, …, 61) corresponding to the wavelength (400, 405, …, 700 nm).

Figure 7 shows the estimation results of the three spectral functions for the pink fluorescent paper samples. The spectral curves of the reflected radiance factor, the emission spectrum, and the excitation spectrum are depicted in Figures 7 (a), 7 (b), and 7 (c), respectively. The Donaldson matrix constructed with the estimated spectral functions was shown in previous Figure 1. The performance index was J=3.5. Figures 8 and 9 show the estimation results for the green fluorescent paper sample. The emission range was estimated to be $17 \le \lambda \le 53$. The estimated curves of the three spectral component functions are depicted in Figure 8. The estimated Donaldson matrix is depicted in Figure 9, where J=14.2.

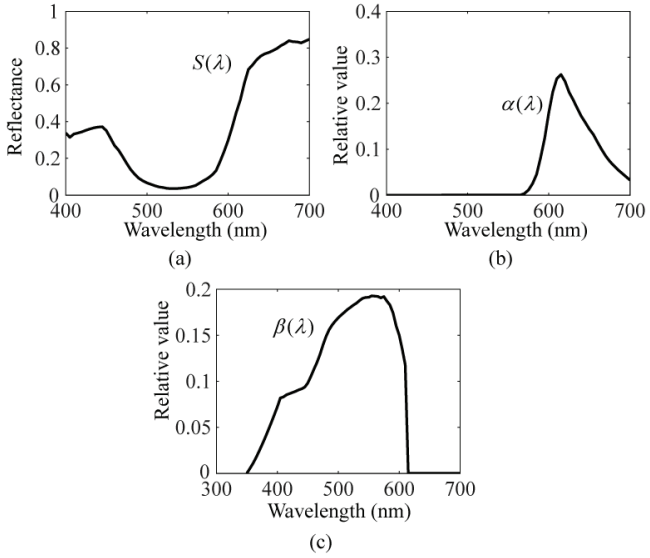

Figure 7 Estimation results of the three spectral function for the pink fluorescent paper samples.(a) Reflected radiance factor, (b) emission spectrum, and (c) excitation spectrum.

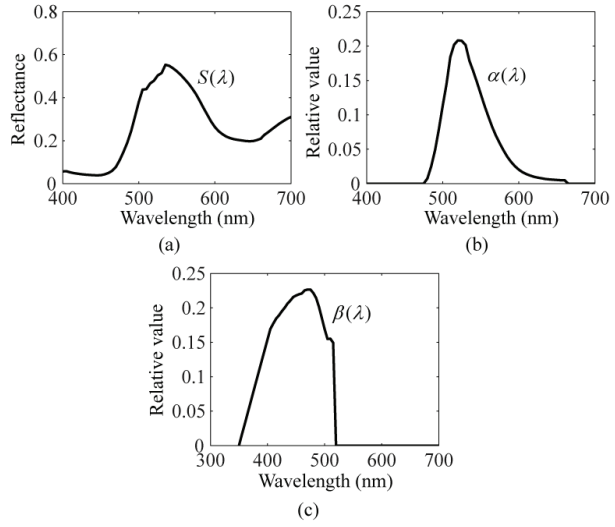

Figure 8 Estimation results of the three spectral function for the green fluorescent paper samples. (a) Reflected radiance factor, (b) emission spectrum, and (c) excitation spectrum.

Figure 10 shows the Donaldson matrix of the green sample estimated by the conventional method, where two light sources of (1) the incandescent lamp and (2) the artificial sunlight lamp were used to illuminate the two samples. It is seen in Figure 10 that the estimated spectral curve of the reflected radiance factor is not smooth. The index value was J=47.3. The index value is much larger than the proposed method.

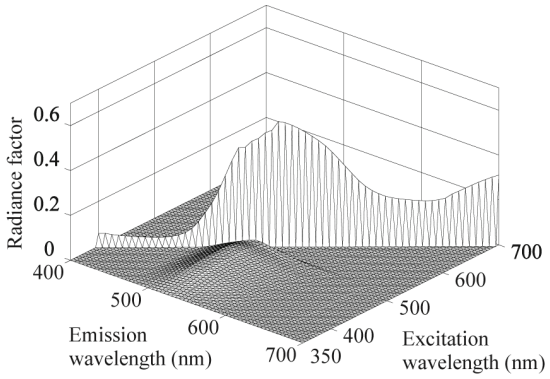

Figure 9 Estimated Donaldson matrix for the green fluorescent paper sample.

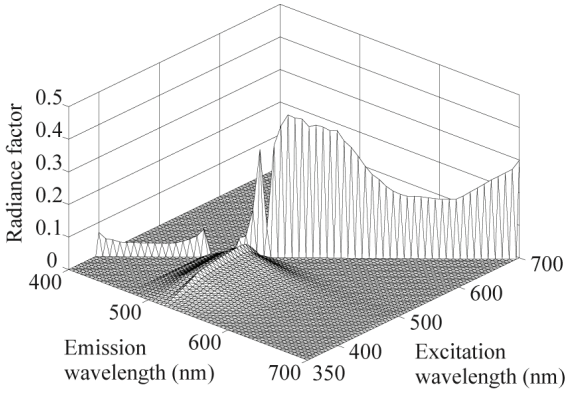

Figure 10 Donaldson matrix for the green fluorescent sample estimated by the conventional method, where two light sources of the incandescent lamp and the artificial sunlight lamp were used.

Conclusions

In this paper, we have proposed a generalized method to estimate the bispectral Donaldson matrices of fluorescent objects. We used two and more light sources. We supposed that the matte surface of a fluorescent object was uniformly illuminated by each light source, and was observed by a spectral imaging system in a visible wavelength range. The Donaldson matrix was decomposed into three spectral components of reflection, fluorescent excitation and fluorescent emission.

A computational algorithm was presented to effectively estimate the three spectral functions. We segmented the output visible wavelength range into two types of ranges: one consisting of only reflection without fluorescent emission and another consisting of both reflection and fluorescent emission. In the former range, the reflection component was straightforwardly estimated and in the latter range, the three components were estimated iteratively to minimize the residual error to multiple observations under different illuminants. The wavelength range of

luminescent emission was also estimated precisely on the residual minimization. The feasibility of the proposed method was confirmed using two fluorescent samples and four illuminants in details.

The proposed method is reliable in the sense that the estimates are determined to minimize the average residual error to the observations obtained over the entire visible wavelength and different illuminants. In this paper, the Donaldson matrix was estimated based on the observations obtained by a spectral imaging system operated in the visible range. The algorithm is not limited to a spectral imaging system but applied to any spectrometer for spectral radiance measurement. We can easily extend the Donaldson matrix to the wider wavelength range of (350, 700 nm) ×(350, 700 nm).

Acknowledgement

This work was supported by Grant-in-Aid for Scientific Research on Innovative Areas (No. 15H05926) from MEXT, Japan.

References

[1] R. Donaldson, Spectrophotometry of fluorescent pigments, British J. of Applied Physics, Vol.5, pp.210-214, 1954.

[2] CIE, Calibration Methods and Photo-Luminescent Standards for Total Radiance Factor Measurements, CIE 182:2007, Commission Internationale de l'Eclairage, Vienna, 2007.

[3] S. Tominaga, K. Hirai, and T. Horiuchi, Estimation of bispectral Donaldson matrices of fluorescent objects by using two illuminant projections, J. Optical Society of America A, Vol. 32, No. 6, pp.1068-1078, 2015.

[4] S. Tominaga, K. Kato, K. Hirai, and T. Horiuchi, Spectral image analysis of mutual illumination between florescent objects, J. Optical Society of America A, Vol. 33, No. 8, pp.1476-1487, 2016.

[5] S. Tominaga, K. Kato, K. Hirai, and T. Horiuchi, Spectral image analysis and appearance reconstruction of fluorescent objects under different illuminations, Proc. 4th CIE Expert Symposium on Colour and Visual Appearance, pp.140-146, Prague, Sep., 2016.

[6] S. Tominaga, K. Kato, K. Hirai, and T. Horiuchi, Appearance decomposition and reconstruction of textured fluorescent objects, Proc. IS&T Inter. Sympo. Electronic Imaging 2017 in the Material Appearance Conference, paper MAAP-290, San Francisco, January, 2017.

[7] J. R. Lakowicz, *Principles of Fluorescence Spectroscopy*, Third ed., Springer, 2006.

[8] M. Mohammadi, *Developing an Imaging Bi-Spectrometer for Fluorescent Materials,* Ph.D. Dissertation, Chester F. Carlson Center for Imaging Science, RIT, 2009.

[9] F. Schieber, Modeling the Appearance of Fluorescent Colors, Proc. Human Factors and Ergonomics Society Annual Meeting, Vol. 45, pp. 1324-1327, 2001.

Author Biography

Shoji Tominaga received the Ph.D. degrees in electrical engineering from Osaka University, Japan, in 1975. In 2006, he joined Chiba University, Japan, where he was a Professor (2006-2013) and Dean (2011-2013) at Graduate School of Advanced Integration Science. He is now a Specially Appointed Researcher, Chiba University, and a Professor at NTNU, Norway. His research interests include multispectral imaging and material appearance. He is a Fellow of IEEE, IS&T, SPIE, and OSA.